

1 **Title**

2 **Precise timing of sensory modulations coupled to eye movements**  
3 **during active vision**

4

5 **Author Information**

6 Christ Devia<sup>1,2,4</sup>, Rodrigo Montefusco-Siegmund<sup>1,2</sup>, José Ignacio Egaña<sup>1,2,3</sup>, and Pedro E.  
7 Maldonado<sup>1,2</sup>.

8 1 Programa de Fisiología y Biofísica, Facultad de Medicina, Universidad de Chile.

9 2 Biomedical Neuroscience Institute, Universidad de Chile.

10 3 Departamento de Anestesiología y Reanimación, Facultad de Medicina, Universidad de  
11 Chile.

12 4 Escuela de Psicología, Pontificia Universidad Católica de Chile, Santiago, Chile.

13

14 The authors declare no competing financial interest.

15

16 **Correspondence:**

17 Dr. Pedro E. Maldonado

18 Facultad de Medicina, Universidad de Chile,

19 Av. Independencia 1027, Independencia, Santiago 8380453, Chile.

20 e-mail: [pedro@neuro.med.uchile.cl](mailto:pedro@neuro.med.uchile.cl)

21

22 **Acknowledgements**

23 This work was made possible in part by a grant from CONICYT,  
24 FONDECYT/Postdoctorado 3140306 to CD and by ICM-P09-015F.

25

26 **Author Contributions**

27 C.D., with comments from R.M.S, J.I.E., and P.E.M., conceived the experiment, and C.D.  
28 and J.I.E. carried out the records; C.D. and R.M.S. designed and carried out the data  
29 analysis with help from J.I.E.; C.D. wrote the paper and R.M.S., J.I.E., and P.E.M.  
30 contributed to its editing.

31

31 **Abstract**

32 **Perception is the result of ongoing brain activity combined with sensory stimuli. In**  
33 **natural vision, changes in the visual input typically occur as the result of self-initiated**  
34 **eye movements. Nonetheless, in most studies, stimuli are flashed, and natural eye**  
35 **movements are avoided or restricted. As a consequence, the neural sensory processing**  
36 **associated with active vision is poorly understood. Here, we show that occipital event-**  
37 **related potentials (ERP) to eye movements during free exploration of natural images**  
38 **exhibited different amplitudes, time course and motor dependency than that from the**  
39 **same flashed stimuli. We found that the ERP to visual fixations doubles in P1**  
40 **magnitude and does not show a late component, which is classically seen with flashed**  
41 **stimuli<sup>1,2</sup>. In addition, we discovered that the ERP to the saccade onset was as large as**  
42 **the ERP to fixations onset, with an early component that preceded the visual input,**  
43 **suggesting that a motor modulation was associated with the saccades<sup>3</sup>. Furthermore,**  
44 **the use of different visual scenes revealed that both the ERP amplitude and time**  
45 **course were dependent on the type of image explored. Our results demonstrated that**  
46 **during active vision, the nervous system engages a mechanism of sensory modulation**  
47 **that is precisely timed to the self-initiated stimulus changes. This mechanism could**  
48 **help coordinate neural activity across different cortical areas and, by extension, serve**  
49 **as a general mechanism for the global coordination of neural networks.**

50

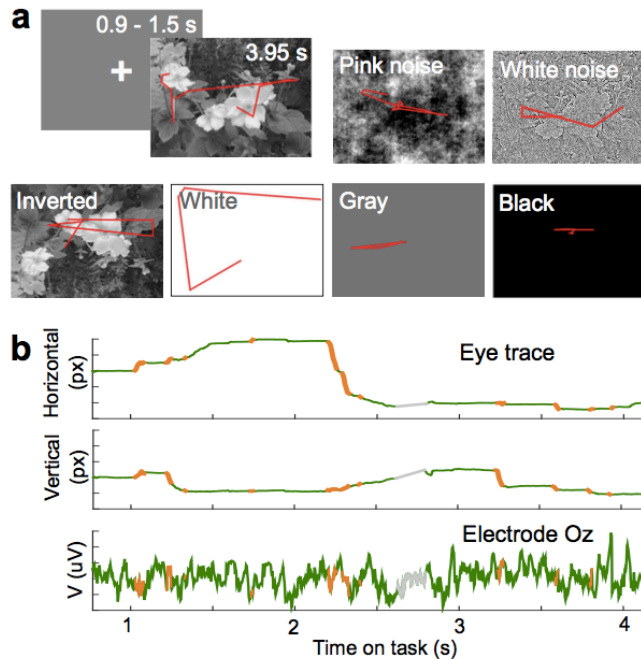
50 **Results**

51 Event-related potentials (ERP) obtained from electroencephalographic (EEG) signals have  
52 been one of the fundamental tools for studying the sensory and cognitive processes in the  
53 brain. Characteristically, these signals represent the average activity resulting from the  
54 repetitive presentation of a stimulus. In most vision studies to date, the stimuli are flashed  
55 in front of subjects, a situation that contrasts with natural vision where subjects, by moving  
56 their eyes, self-initiate changes in the visual input. Although saccade (saccRP), fixation  
57 (fixRP), and image (imgRP) related potentials have been independently explored<sup>1,4-6</sup>, the  
58 neuronal processes that underlie these different responses are not well understood. We  
59 hypothesize that a direct comparison of these responses would reveal distinct mechanisms  
60 involved in passive and active vision.

61 In this work, we assessed the magnitude of the modulation by self-driven eye movements  
62 on the activity in the early visual areas in human subjects. During each trial, the subjects  
63 freely explored pictures (Fig. 1a) while their eye movements and EEG activity were  
64 recorded (Fig. 1b). The subjects (n = 16) freely explored natural scenes (NS) and 6 other  
65 control categories (pink noise, white noise, and white, grey, and black images; Fig. 1a).

66

67



68

69 **Figure 1| Free-viewing task, eye movements and EEG recordings. a.** The subjects freely  
70 explored images from 7 categories (natural scenes, pink noise, white noise, inverted scenes,  
71 and white, grey, and black images). Over an example image is the eye trace (red) of one  
72 subject in all the image categories tested. This example image was not part of the database.  
73 **b.** The time course of the horizontal (Hor) and vertical (Ver) component of the eye  
74 movement, and simultaneous EEG recording (bottom) for the eye trace in the NS of **a.**  
75 Epochs drawn in green, orange, and grey show fixation, saccade, and blinks, respectively.

76

77

78 We first compared the event related potential to the fixation onset with the potential to  
79 image onset (fixRP vs. imgRP). The fixRP exhibited a significantly larger amplitude and a  
80 shorter latency than the imgRP (Fig. 2a), with its maximum amplitude observed in the

81 occipital electrodes (O1, Oz, and O2; see the topography plot in Fig. 2a). Therefore, all  
82 following analyses were performed on the average of those three electrodes. A prominent  
83 positive first peak characterized the fixRP, which was preceded and followed by brief and  
84 small negative potentials. The fixRP waveform was consistent with high frequency power  
85 from the electrocorticogram recordings in the early visual areas in humans<sup>1</sup> (mainly V1,  
86 V2, and V3) and the firing rate in non-human primates<sup>2</sup> (V1, V2, and V4) during free  
87 viewing tasks, suggesting that the EEG probes over the occipital areas were mainly  
88 recording the firing rate on the visual cortex. The positive component (fixP1, latency  $88.10$   
89  $\pm 8$  ms and mean peak amplitude  $5.48 \pm 2.91$   $\mu\text{V}$ ) was visible on each subject, and its  
90 waveform was consistent between the subjects, showing only amplitude modulation. An  
91 additional feature of the fixRP was the negative potential previous to the fixP1 that started  
92 even before the fixation (onset around  $-76.04 \pm 33.65$  ms, min amplitude  $-1.34 \pm 0.77$   $\mu\text{V}$  at  
93  $12.71 \pm 18.94$  ms; Fig. 2a). It has been shown that this negative potential is linearly  
94 modulated by the contrast between successive fixations and nonlinearly by the duration of  
95 the fixation<sup>1</sup>. Because this potential begins before fixation, it suggests that the brain events  
96 related to current stimulus processing on the sensory surface started during the saccade. The  
97 second negative potential that followed fixP1 had even less amplitude ( $-1.46$   $\mu\text{V}$  at 140  
98 ms), and its amplitude is modulated by the fixation duration<sup>1</sup>. As previously reported<sup>6</sup>, the  
99 image related potential (imgRP) exhibited two positive peaks, where the first peak had a  
100 smaller amplitude than the fixRP (the imgP1 mean peak amplitude on NS was  $2.47 \pm 2.87$   
101  $\mu\text{V}$  and the peak latency was  $105.40 \pm 15.6$  ms), and the second potential had a longer

102 duration and amplitude similar to the fixP1 (the imgP2 mean area under the curve was  
103  $299.01 \pm 181.12 \mu\text{Vms}$  and the peak latency was approximately 210 ms). The imgP1  
104 amplitude correlates with the stimulus contrast<sup>3</sup>, and its origin is probably in the dorsal  
105 extrastriate cortex<sup>7</sup>. The second potential on the imgRP, the imgP2, has been proposed to  
106 correspond to the neural correlate of the gist of the scene<sup>6,8</sup>, where the recognition of the  
107 main features of the image may occur<sup>9</sup>. The time course of the fixRP and the imgRP  
108 substantially differed. The fixP1 peaked significantly earlier than the imgP1 (Fig. 2a, left  
109 insert), and despite the large luminance changes that occur at the image onset, the fixP1 had  
110 a significantly larger amplitude than the imgP1 (Fig. 2a, right insert). We demonstrate that  
111 self-triggered changes in the visual stimulus, generated by the exploratory eye-movements,  
112 correlate with a modulation of EEG signals in the human visual cortex that is stronger than  
113 the activity evoked by the onset of the NS image.

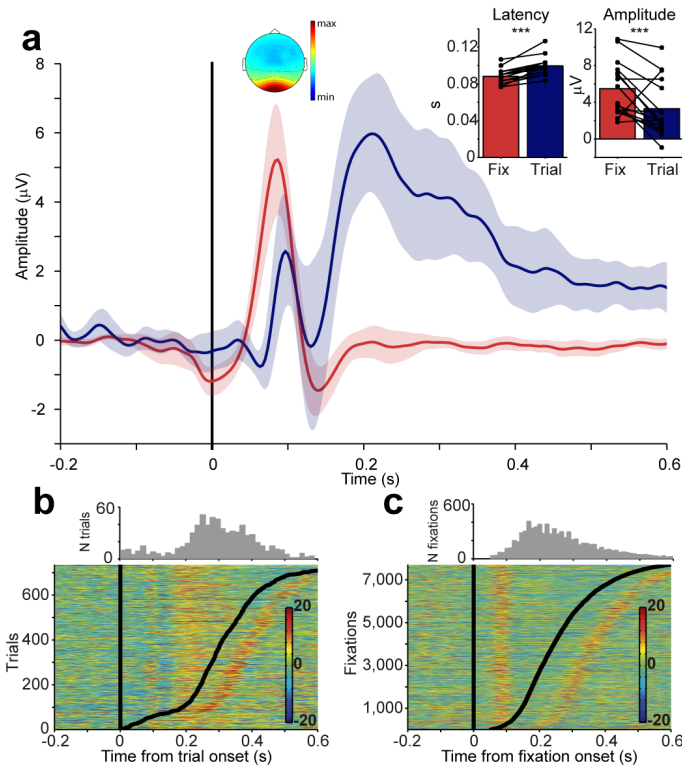
114

115 Previous work on non-human primates showed that the first eye movement is typically  
116 suppressed until 200 ms after image onset<sup>10</sup>. Consequently, we investigated the time of  
117 occurrence of the first fixations after image onset and examined its contribution to imgP2.  
118 Specifically, we determined whether this signal corresponded solely to evoked activity by  
119 the image or was combined with a putative response to the first eye movement after image  
120 onset. As expected, we found that from the 735 first fixations examined, 15.24% occurred  
121 in the first 200 ms after image onset, while 64.63% first fixations occurred during the  
122 period 200-400 ms after image onset (histograms on Fig. 2b, c). All trials were then sorted

123 by the latency of the first fixation (Fig. 2b). We found that the imgP2 component precedes  
124 the increment in the number of first fixations (>200 ms). Moreover, the imgP2 positive  
125 potential was clearly distinguishable from the subsequent fixP1, and it exhibited a longer  
126 duration (the black curved line depicts the fixation onset in Fig. 2b). In contrast, when the  
127 single-trial of fixRP was sorted by the latency to the next fixation (Fig. 2c), the fixP1  
128 potential (the black curved line in Fig. 2c) exhibited a shorter and precise time course, and  
129 we did not observe a second peak regardless of the fixation duration. These results suggest  
130 that the fixRP and the imgRP originate on different brain processes, where the fixRP is  
131 locked to the self-paced eye movement, while imgRP is mostly evoked by stimulus onset  
132 associated with gist and other high-level cognitive processes<sup>6,11,12</sup>.

133

134



135

136 **Figure 2 | Fixation-related potentials exhibit different amplitudes and time courses**

137 **than image-evoked occipital potentials on natural scenes. a.** The occipital evoked

138 response for NS aligned to the fixation onset (red) and image onset (blue). The shadowing

139 depicts confidence intervals. The occipital distribution of fixP1 is over the scalp topography

140 (average over 43 to 117 ms). Left panel, the mean latency of fixP1 and imgP1 (latency of

141 fixP1 vs. latency of imgP1,  $t_{15} = -7.84$ ,  $P = 1.1 \times 10^{-6}$ , paired  $t$ -test). Right panel, mean

142 amplitude of fixP1 and imgP1 across subjects (peak amplitude of fixP1 versus imgP1,  $t_{15} =$

143 3.12,  $P = 0.007$ , paired  $t$ -test). The dots represent each subject during each condition

144 connected by lines. **b.** Top: The histogram shows the distribution of latencies to the first

145 fixation on the image. Bins of 15 ms. Bottom: The single-trials from imgRP aligned to the



146 image onset and sorted by the first fixation latency (black curved line). c. Top: The  
147 histogram shows the distribution of the next fixation latency. Bins of 11 ms. Bottom: The  
148 single-trials activity of fixRP aligned to the fixation onset and sorted by the next fixation  
149 latency (black curved line).

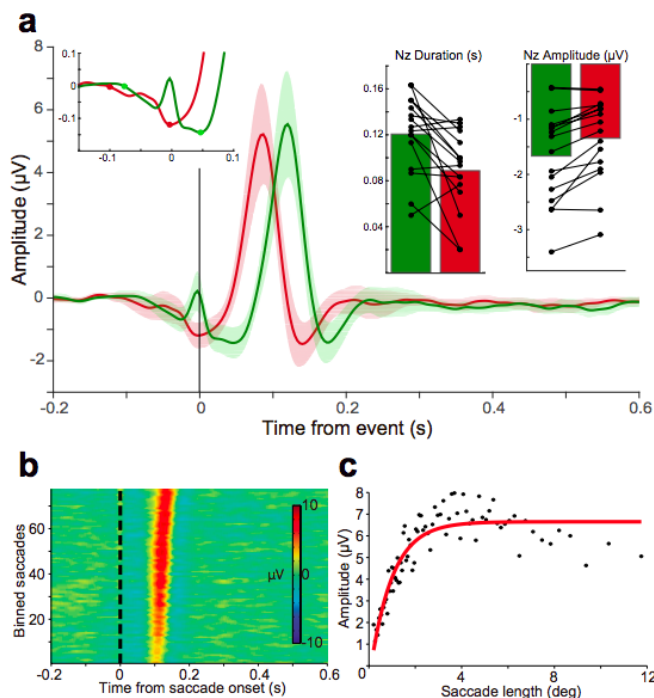
150

151

152 A key feature of active vision is that the self-initiation of a saccade results in an ensuing  
153 and timely visual stimulation. In the primary visual cortex, it has been shown that the local  
154 field potential displays greater amplitude when the signals are aligned to the onset of the  
155 saccades, suggesting an influence of these motor actions in V1 activation<sup>4</sup>. Here, we found  
156 that the saccade related potential (saccRP) presented a negative potential that started before  
157 saccade onset, followed by a positive potential that was larger in amplitude than the fixP1  
158 and that it had a nonlinear modulation by the saccade amplitude. The saccRP (Fig. 3a) had  
159 a negative component that started before saccade onset, which we termed Nz (Negative-  
160 zero). This component was followed by a positive potential (saccP1) that peaked after  
161 saccade onset and ended in another negative deflection. The shape of the saccRP, especially  
162 the saccP1 and the following negativity, resembles the event related potential from the  
163 electrocorticogram recordings in areas V1 and V4<sup>13</sup> and the firing rate on V1<sup>5</sup> in monkeys.  
164 Our data revealed that the Nz was also visible in the fixRP but had significantly reduced  
165 amplitude than in the saccRP ( $-1.67 \pm 0.86 \mu\text{V}$  at  $48.75 \pm 15.09 \text{ ms}$ ; Fig. 3a and inset). The  
166 duration of the Nz, from its onset until the minimum value before P1, was significantly

167 longer than in the fixRP (Fig. 3a, right inset). The Nz also showed a spike potential  
168 coincident with the saccade initiation and duration, and thus, likely originated in the  
169 extraocular muscles that move the eyeball<sup>14-16</sup>. This shows that the spike potential captured  
170 the muscle twitch artefact and that this muscle activity was distinguishable from the  
171 occipital neuronal processes. The amplitude of the saccP1 ( $6.02 \pm 3.23 \mu\text{V}$  at  $120 \pm 8.5$  ms)  
172 was significantly larger than that of the fixP1 (Fig. 3a), and peaked 36 ms after the fixP1, a  
173 time lapse coincident with the median duration of saccades<sup>17</sup> (here, the median saccade  
174 duration was 31.98 ms, with 10 ms and 60 ms at 5% and 95% of the distribution,  
175 respectively). These results for the Nz and saccP1 show that brain activity from occipital  
176 areas is larger in amplitude and better timed to the saccade onset rather than to the fixation  
177 onset. We conclude that saccades are instrumental in modulating the visual processing of  
178 the subsequent foveated visual patches. For short saccade lengths, the amplitude of the  
179 saccP1 increased with the amplitude of the movement (Fig. 3b), showing a linear  
180 correlation for saccades smaller than  $2.5^\circ$  (Fig. 3c), which is intriguingly within the fovea  
181 size range (the foveal diameter is approximately  $5^\circ$ ). However, for saccades larger than the  
182 fovea radius, the saccP1 amplitude seems to saturate regardless of the saccade length (Fig.  
183 3c). These findings demonstrate that this component of the response cannot be of purely  
184 motor origin because otherwise, its amplitude should keep growing linearly with the  
185 saccade length. Additionally, the relationships between saccade length, foveal size, and  
186 saccP1 support previous studies that reported that humans and monkeys employ ambient  
187 and focal modes of visual exploration while freely viewing natural scenes<sup>18,19</sup>. Finally, the

188 negative potential that came after the saccP1 was similar between the saccRP and fixRP.  
189 This potential is coincident with the suppression of the firing rate in V1 for small saccades<sup>5</sup>,  
190 which is absent when the movement is externally induced instead of self-initiated.  
191 Together, these results demonstrate that during free viewing of NS, the processing of the  
192 upcoming stimulus in the early visual areas is timed to the saccade onset and that saccade-  
193 related brain activity contributes to the processing of visual images.  
194  
195



196  
197 **Figure 3 | The saccade related potential (saccRP) is larger than the fixRP and exhibits**  
198 **an early component that is differentially modulated by short and long saccades. a** The  
199 saccRP (green) and fixRP (red) are plotted on the same time axes. The saccP1 was bigger

200 than the fixP1 ( $t_{15} = -2.75$ ,  $P = 0.02$ , paired  $t$ -test). Time zero is the event onset, saccade or  
201 fixation, respectively. The shaded area is the confidence interval. Inset: The details on the  
202 Nz, the negative potential that started before the saccade onset. The dots over the curves  
203 denote the landmarks used to measure Nz duration. Inset, left: The bar plot shows the  
204 duration of the Nz on the saccRP and fixRP (saccRP  $120.63 \pm 33.82$  ms, Nz<sub>fix</sub> vs. Nz<sub>sacc</sub>  $t_{15}$   
205  $= -3.47$ ,  $P = 0.003$ , paired  $t$ -test). Inset, right: The Nz has a larger amplitude on the saccRP  
206 than on the fixRP (Nz amplitude on the fixRP versus the saccRP,  $t_{15} = -4.50$ ,  $P = 4.26 \times 10^{-4}$ ,  
207 paired  $t$ -test). The dots represent each subject on each condition connected by lines. **b.** The  
208 mean EEG activity on bins based on saccade length. Each bin is the average of 100 trials  
209 previously sorted by saccade length. **c.** The mean saccP1 and mean saccade length on  
210 binned data from b (Correlation for saccade length  $\leq 2.5^\circ$  was  $\rho = 0.93$ ,  $P = 0$ ; for longer  
211 saccades  $\rho = -0.22$ ,  $P = 0.19$  Spearman correlation).

212

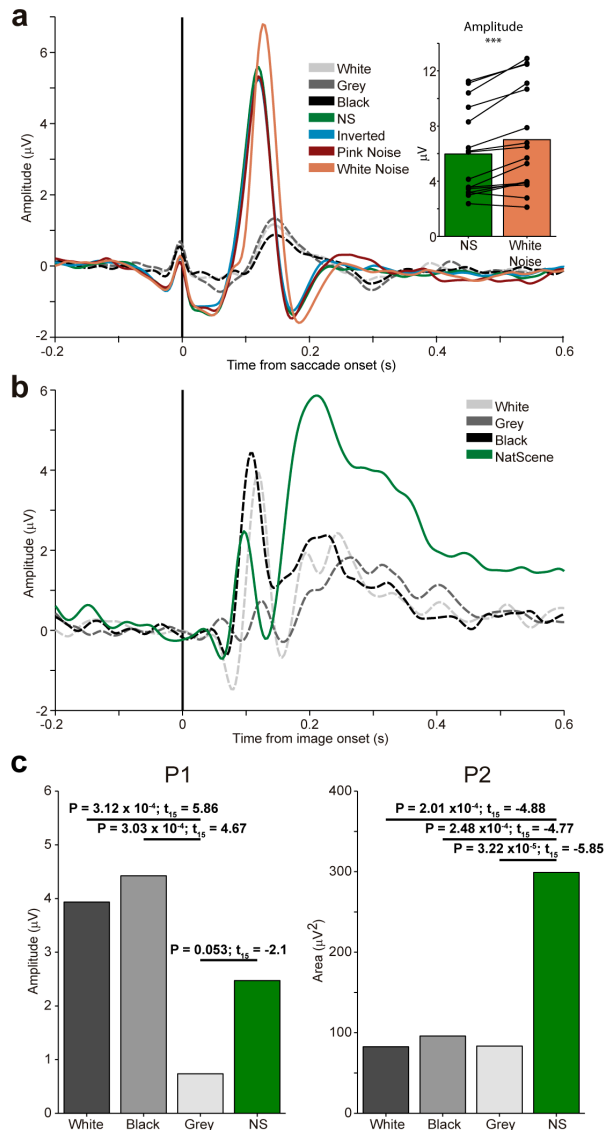
213

214 Previous studies have shown that the fixRP is modulated by the luminance contrast  
215 between two fixation points<sup>20</sup>. To further investigate how low-level features of visual  
216 scenes modulate the saccRP, we measured the saccRP in plain (white, black and grey  
217 images) and textured images (pink noise, white noise, and inverted images, see the Methods  
218 section and Fig. 1a) and found that the saccRP also depended on the content of the image  
219 (Fig. 4a). The saccRP on the plain images showed a smaller and delayed development of a  
220 positive deflection approximately 150 ms after saccade onset, which is in contrast with the

221 well-defined saccP1 on NS. As a group, the textured images showed a significantly larger  
222 amplitude of Nz compared with the plain images. Similarly, the saccP1 amplitude was  
223 significantly increased in the textured images compared with the plain images. Specifically,  
224 the saccRP in the plain images had a reduced Nz ( $-0.57 \pm 0.44$ ; white  $-0.45 \pm 0.40 \mu\text{V}$ ,  
225 black  $-0.46 \pm 0.43 \mu\text{V}$ , grey  $-0.79 \pm 0.52 \mu\text{V}$ ), and the saccP1 was almost absent (white  
226  $0.60 \pm 0.99 \mu\text{V}$ , black  $0.50 \pm 0.91 \mu\text{V}$ , grey  $0.69 \pm 0.83 \mu\text{V}$ ). These reduced potentials on  
227 plain images are in accordance with a general reduction in the firing rate on V1 when a  
228 grey screen is on the receptive field of monkeys<sup>5</sup>. In contrast, for textured images (pink  
229 noise, white noise, and inverted images), we found that the Nz and the saccP1 were  
230 conserved and had similar magnitudes to NS potentials. The Nz potential was similar across  
231 the textured categories (NS  $-1.62 \pm 0.73 \mu\text{V}$ , pink noise  $-1.39 \pm 0.71 \mu\text{V}$ , white noise  $-1.45$   
232  $\pm 0.81 \mu\text{V}$ , inverted images  $-1.32 \pm 0.67 \mu\text{V}$ ). These large differences in Nz signals cannot  
233 be attributed to motor modulation because the subjects still produce eye movements in  
234 plain as in textured images. The saccP1 amplitude was similar between the NS ( $6.02 \pm 3.23$   
235  $\mu\text{V}$ ), pink noise ( $5.68 \pm 3.29 \mu\text{V}$ ), and inverted images ( $5.57 \pm 3.02 \mu\text{V}$ ; Fig. 4a inset).  
236 Notably, the white noise images elicited the largest saccP1 amplitude<sup>21</sup> ( $7.11 \pm 3.84 \mu\text{V}$ ),  
237 even larger than the NS images. This latter result can be explained, in part, by the change in  
238 luminance between two successive fixations<sup>20</sup>. However, it can also be interpreted as a  
239 decrement in the predictability of the content of the next fixation<sup>22</sup>. Further examination of  
240 the saccP1 and its relation with saccade length supports this latter hypothesis, where the  
241 linear relation between the saccP1 and saccade length exhibited a steeper slope for the

242 white noise images than the NS images. This would also explain our findings of  
243 significantly smaller saccP1 amplitudes for the plain images, given that there is no  
244 luminance contrast between successive fixations and full predictability of the content of the  
245 next fixation. A putative explanation to conciliate the reduction in both Nz and sacP1 in the  
246 plain images would suggest that as quickly as the gist of the image is acquired after image  
247 onset, a distinct visual process ensues, which would depend on the nature of the gist. As a  
248 result, on plain image presentations, the motor-related modulation observed in the textured  
249 images may not be engaged, as subjects quickly perceive a uniform visual scene. However,  
250 for the textured images, each eye movement resulted in a new stimulus to early visual areas  
251 that needed to be processed. Thus, motor-related modulation becomes an important part of  
252 the visual processing of each fixation. This conjecture is consistent with our finding that the  
253 Nz and saccP1 on the plain images were not due to some lack of general response to the  
254 stimulus. Indeed, when we examined the response to the onset of the images, we verified  
255 that plain images were able to produce the expected imgP1 component and a weak imgP2,  
256 with similar timing to imgRP on NS (Fig. 4b). There were significant differences for the  
257 imgP1 between the plain and NS categories (NS, white, grey, and black). The transition  
258 from the fixation cross (grey background during the inter-trial interval; Fig. 1a) to the grey  
259 images evoked an imgP1 of smaller amplitude than in the NS (grey  $0.74 \pm 1.45 \mu\text{V}$  and NS  
260  $2.47 \pm 2.87 \mu\text{V}$ ), and for white and black images, the imgP1 was larger than in the NS ( $3.93$   
261  $\pm 2.69 \mu\text{V}$  and  $4.42 \pm 3.69 \mu\text{V}$ , respectively), but not significantly. The imgP1 was  
262 significantly larger for the white and black images than the grey. These results, as with the

263 NS images (Fig. 2a), further indicate that the imgP1 was mainly modulated by the  
264 difference in luminance between the current and the previous image<sup>3</sup>. The late component,  
265 imgP2, also had significant differences between categories (Fig. 4b). The imgP2 was  
266 similar between the plain images (white  $82.53 \pm 104.84 \mu\text{V}$ , black  $95.91 \pm 90.54 \mu\text{V}$ , and  
267 grey  $83.52 \pm 74.89 \mu\text{V}$ ), and significantly smaller than the NS ( $299.01 \pm 181.12 \mu\text{V}$ ). These  
268 results further support the interpretation of imgP2 as the correlate of the gist of the scene<sup>6</sup>.  
269  
270



271

272 **Figure 4 | The saccRP and imgRP on plain and complex images. a.** The saccRP on plain  
 273 (white, grey, and black) and complex images (NS, inverted, pink noise, and white noise; Nz  
 274 from all content images versus all plain images,  $t_{15} = -4.84$ ,  $P = 2.18 \times 10^{-4}$ , paired  $t$ -test; the  
 275 same for saccP1,  $t_{15} = 7.55$ ,  $P = 1.74 \times 10^{-6}$ , paired  $t$ -test). Inset, the white noise saccP1  
 276 compared with the NS ( $t_{15} = -5.01$ ,  $P = 1.53 \times 10^{-4}$ , paired  $t$ -test). **b.** The imgRP on the NS



277 and plain images (imgP1,  $F_{3,45} = 7.75$ ,  $P = 2.79 \times 10^{-4}$ ; imgP2,  $F_{3,45} = 21.60$ ,  $P = 8.17 \times 10^{-9}$ ,  
278 one-way ANOVA repeated measures). c. Left: A bar plot of imgP1 amplitude in the NS  
279 and plain images. No significant differences between NS and grey ( $P = 0.46$ ) or between  
280 white or black images and NS ( $P = 0.16$  and  $P = 0.09$ , respectively). Right: A bar plot of the  
281 imgP2 amplitude in the NS and plain images. ( $P = 0.53$  white vs. black,  $P = 0.96$  white vs.  
282 grey,  $P = 0.50$  black vs. grey). A paired  $t$ -test was carried out for all bar plots.

283

284

## 285 CONCLUSIONS

286 Our results show that during self-paced image exploration, the activity in the brain occipital  
287 areas is time-modulated to the saccade onset rather than to the fixation onset. The evoked  
288 activity to the saccade onset (saccRP) has increased amplitude compared to the activity  
289 evoked by the fixation onset. Moreover, these potentials were greater in magnitude than the  
290 response to image onset. Our results provide additional evidence of the role of internally  
291 generated motor signals in the modulation of neural activity in early visual areas<sup>4</sup> and  
292 suggest that self-initiated sensory activity triggers different neural processes than those  
293 triggered from externally imposed stimuli. Another important finding was that the  
294 amplitude of the saccP1 for the natural scenes is linearly correlated with saccade length that  
295 fall within the fovea radius. This result fits well with the idea of a local-global strategy  
296 working during free visual exploration<sup>19,23</sup>. Additionally, we found that the saccRP is  
297 almost absent for images without texture (plain images), even though subjects still move

298 their eyes. A possible explanation for this latter result is that the internally generated motor  
299 signal is not engaged during exploration of the plain images. This implies that, shortly after  
300 image presentation, the perceptual process categorizes images as plain or textured. As  
301 expected, the imgP2 depends on the class of visual stimulus and was diminished for non-  
302 textured images, supporting imgP2's role in the assessment of scene content. This finding  
303 extends previous reports proposing that the imgP2 is the neural correlate of the gist of an  
304 image<sup>6</sup>.

305 Altogether, our results suggest that during image exploration, two different modes that are  
306 mutually exclusive can be engaged. A sensory motor modulation over early visual cortex  
307 acts when the explored scene has textures, but it is disengaged when an image is  
308 categorized as plain. The findings from this research have important implications for  
309 classical paradigms in visual neuroscience, where stimuli are flashed to the subjects in an  
310 externally paced frequency and highlights the need to complement the current body of  
311 literature with free exploration paradigms, where intrinsic brain processes are exposed. We  
312 should ask not what the brain can do but what the brain actually does.

313

313 **Methods**

314 **Subjects.** A total of 16 subjects participated in this experiment (5 female); 13 were right-  
315 handed, 8 had right ocular dominance, and their average age was  $31.41 \pm 7.17$  years. All  
316 have normal or corrected-to-normal vision. All subjects were volunteers and accepted to  
317 participate through a written informed consent; the consent form and all experimental  
318 protocols were approved by the Ethics Committee for Research in Humans of the Faculty  
319 of Medicine from Universidad de Chile. All recordings were performed within a 32-day  
320 period.

321 **Stimuli and task.** A total of 46 natural images, from the International Affective Picture  
322 System (IAPS)<sup>24</sup>, were selected based on their valence and arousal value, with all ranging  
323 in the middle values of the database (mean valence  $6.62 \pm 1.09$ ; mean arousal  $4.08 \pm 0.96$ ).  
324 The selected images were gamma corrected for the screen used to present the stimuli, and  
325 these images constituted the NS set. For each of the NS images, we constructed 4 control  
326 images: pink noise, white noise, inverted, and grey. The pink noise and white noise images  
327 were created considering 2 parameters of the NS – its power spectrum and its phase. The  
328 pink noise images had the same spectral power as that of the NS, with the phase from a  
329 scrambled version of the original NS. As a complement, the white noise images were  
330 created having a flattened power spectrum of the scrambled version of the NS and the  
331 phase content of the original NS. The inverted images were created as a high-level control,  
332 where they were the original NS upside down with the bottom part at the top the image.  
333 The grey images had the same average luminance as that of the original NS. Finally, the

334 white and black images were also created as controls of the luminance, and they had the  
335 maximum ([255,255,255] RGB) and minimum luminance ([0,0,0] RGB), respectively. The  
336 subjects' eyes were 70 cm from the screen. The screen size was 1920 (width) x 1080  
337 (height) pixels, and the mean 32 pixels per cm was equivalent to 39.38 pixels per visual  
338 degree. The image size was 1024 x 768 pixels, and it was centred on the screen. The  
339 remaining borders in the screen were a plain grey colour ([173,173,173] RGB). The  
340 subjects were seated in a dark room with their chin rested. We first recorded a couple of  
341 minutes of the EEG while the subjects rested (data not analysed here). Then, they  
342 performed the main task where they were instructed to explore the images freely, as there  
343 would be questions about their content at the end. Here, a total of 322 images divided into 2  
344 blocks were presented. Finally, on a third task, they observed 54 images, where 8 were not  
345 part of the main task, and they were asked whether they remembered seeing the image.

346 **Recordings.** We recorded the brain activity using 32 electrodes (ActiveTwo, BioSemi,  
347 Amsterdam, The Netherlands) displayed as in the International 10-20 system. In addition,  
348 eight electrodes, one on each mastoid for re-referencing, while the other six recorded the  
349 electro-oculogram (EOG), were placed above, below, and on the outer canthi of each eye.  
350 The EEG and EOG were recorded at 2048 Hz. The gaze position and pupil diameter were  
351 recorded with a chin rest eye tracking system at 1000 Hz (EyeLink 1000, SR-Research,  
352 ON, Canada).

353 **Eye movement analysis.** For all analyses of eye movements, we considered only the data  
354 obtained for the right eye. The saccades and fixations were automatically detected based on

355 the velocity ( $30^\circ/\text{s}$ ) and acceleration threshold ( $8000^\circ/\text{s}^2$ ). The saccades longer than 5 ms  
356 and smaller than 100 ms and the fixations between 50 and 600 ms were considered for  
357 further processing. The blinks were defined as the absence of pupil data. The saccades that  
358 were actually blinks were discarded (a median of 9.32% of the events were blinks).

359 **EEG and ERP analyses.** The EEG processing was done in Matlab (release 2012b; The  
360 MathWorks, Inc., Natick, Massachusetts, United States) using the toolbox FieldTrip  
361 (release 20140412)<sup>25</sup>. The recordings were re-referenced to the average of the mastoids.  
362 Then, we performed an ICA decomposition of the data<sup>26</sup> and visually compared the EOG  
363 channels with the ICA components to discard the ICA components that had ocular content  
364 from the remaining components, and we reconstructed the signal. Then, the data were  
365 decimated to a sample rate of 300 Hz. We applied a band-pass filter (Butterworth) between  
366 0.5 and 30 Hz. The epochs were defined 1 second before the event onset until 1 second  
367 after. We used the period [-200, -100] ms as baseline for fixRP and saccRP and between [-  
368 200, 0] ms for imagRP. We studied the average event-related potentials from the occipital  
369 electrodes (O1, Oz, and O2) time-locked to fixation, saccade, or image onset, respectively.  
370 For each subject, we assessed the peak amplitude of these potentials, while for imgP2, we  
371 considered the area under the curve. We used the area under the curve because it was not  
372 possible to detect a clear maximum for the imgP2 of each subject<sup>27</sup>. The onset of Nz was  
373 defined as the first point between [-100,+100] ms, where three consecutive samples were  
374 below the baseline. The offset was the point where the saccRP reached a minimum, just  
375 before the positive deflection of saccP1 began.

376 **Statistics.** We measured the significant differences for fixRP *versus* imgRP, and fixRP  
377 *versus* saccRP with paired *t*-tests. The subjects were the independent samples, and we  
378 reported the *t*-statistics, with its degrees of freedom, and P-value. We applied the test over  
379 the maximum or minimum amplitude of the potentials (for sacc/fix/imgP1 and sacc/fix Nz,  
380 respectively) and the area under the curve for imgP2. To assess the significant differences  
381 across image categories, we performed an ANOVA of repeated measures and reported the  
382 F-statistic of times (image categories), with the degrees of freedom of the times and error  
383 ( $F_{df_{\text{Times}}, df_{\text{Error}}}$ ), along with its P-value.  
384

384 **References**

- 385
- 386 1. Podvalny, E., Yeagle, E., Mégevand, P., Sarid, N. & Harel, M. Invariant Temporal  
387 Dynamics Underlie Perceptual Stability in Human Visual Cortex. *Current Biology*  
388 (2016).
- 389 2. Gallant, J. L., Connor, C. E. & Van Essen, D. C. Neural activity in areas V1, V2 and  
390 V4 during free viewing of natural scenes compared to controlled viewing.  
391 *Neuroreport* (1998).
- 392 3. Johannes, S., Münte, T. F., Heinze, H. J. & Mangun, G. R. Luminance and spatial  
393 attention effects on early visual processing. *Brain Res Cogn Brain Res* **2**, 189–205  
394 (1995).
- 395 4. Ito, J., Maldonado, P. & Grün, S. Cross-frequency interaction of the eye-movement  
396 related LFP signals in V1 of freely viewing monkeys. *Front Syst Neurosci* **7**, 1  
397 (2013).
- 398 5. Troncoso, X. G. *et al.* V1 neurons respond differently to object motion versus  
399 motion from eye movements. *Nat Commun* **6**, 8114 (2015).
- 400 6. Harel, A., Groen, I. I. A., Kravitz, D. J., Deouell, L. Y. & Baker, C. I. The Temporal  
401 Dynamics of Scene Processing: A Multifaceted EEG Investigation. *eNeuro* **3**,  
402 (2016).
- 403 7. Di Russo, F., Martínez, A., Sereno, M. I., Pitzalis, S. & Hillyard, S. A. Cortical  
404 sources of the early components of the visual evoked potential. *Hum Brain Mapp* **15**,  
405 95–111 (2002).
- 406 8. Thorpe, S., Fize, D. & Marlot, C. Speed of processing in the human visual system.  
407 *Nature* (1996).
- 408 9. Oliva, A. & Torralba, A. Building the gist of a scene: the role of global image  
409 features in recognition. *Prog. Brain Res.* **155**, 23–36 (2006).
- 410 10. Bartlett, A. M., Ovaysikia, S., Logothetis, N. K. & Hoffman, K. L. Saccades during  
411 object viewing modulate oscillatory phase in the superior temporal sulcus. *J.*  
412 *Neurosci.* **31**, 18423–18432 (2011).
- 413 11. Devillez, H., Guyader, N. & Guérin-Dugué, A. An eye fixation-related potentials  
414 analysis of the P300 potential for fixations onto a target object when exploring  
415 natural scenes. *Journal of Vision* **15**, 20 (2015).
- 416 12. Villena-González, M., López, V. & Rodriguez, E. Orienting attention to visual or  
417 verbal/auditory imagery differentially impairs the processing of visual stimuli.  
418 *Neuroimage* **132**, 71–78 (2016).
- 419 13. Brunet, N. *et al.* Visual cortical gamma-band activity during free viewing of natural  
420 images. *Cereb. Cortex* **25**, 918–926 (2015).
- 421 14. Kautz, L. N. *et al.* Looking for a face in the crowd: fixation-related potentials in an  
422 eye-movement visual search task. *Neuroimage* **89**, 297–305 (2014).
- 423 15. Ioannides, A. A., Fenwick, P. B. C. & Liu, L. Widely distributed  
424 magnetoencephalography spikes related to the planning and execution of human  
425 saccades. *J. Neurosci.* **25**, 7950–7967 (2005).

- 426 16. Carl, C., Aık, A., Konig, P., Engel, A. K. & Hipp, J. F. The saccadic spike artifact  
427 in MEG. *Neuroimage* **59**, 1657–1667 (2012).
- 428 17. Bahill, A. T., Clark, M. R. & Stark, L. The main sequence, a tool for studying human  
429 eye movements. *Mathematical Biosciences* (1975).
- 430 18. Borji, A. & Itti, L. State-of-the-art in visual attention modeling. *IEEE Trans Pattern*  
431 *Anal Mach Intell* **35**, 185–207 (2013).
- 432 19. Ito, J. *et al.* Switch from ambient to focal processing mode explains the dynamics of  
433 free viewing eye movements. *Sci Rep* **7**, 1082 (2017).
- 434 20. Ossandon, J. P., Helo, A. V., Montefusco-Siegmund, R. & Maldonado, P. E.  
435 Superposition model predicts EEG occipital activity during free viewing of natural  
436 scenes. *J. Neurosci.* **30**, 4787–4795 (2010).
- 437 21. Katz, L. N., Yates, J. L., Pillow, J. W. & Huk, A. C. Dissociated functional  
438 significance of decision-related activity in the primate dorsal stream. *Nature* **535**,  
439 285–288 (2016).
- 440 22. Rao, R. P. & Ballard, D. H. Predictive coding in the visual cortex: a functional  
441 interpretation of some extra-classical receptive-field effects. *Nat. Neurosci.* **2**, 79–87  
442 (1999).
- 443 23. Berger, D. *et al.* Viewing strategy of Cebus monkeys during free exploration of  
444 natural images. *Brain Research* **1434**, 34–46 (2012).
- 445 24. Lang, P. J., Bradley, M. M. & Cuthbert, B. N. *International affective picture system*  
446 *(IAPS): Affective ratings of pictures and instruction manual*. (Technical report A-8,  
447 2008).
- 448 25. Oostenveld, R., Fries, P., Maris, E. & Schoffelen, J.-M. FieldTrip: Open source  
449 software for advanced analysis of MEG, EEG, and invasive electrophysiological  
450 data. *Comput Intell Neurosci* **2011**, 156869 (2011).
- 451 26. Comon, P. Independent component analysis, a new concept? *Signal processing*  
452 (1994).
- 453 27. Picton, T. W. *et al.* Guidelines for using human event-related potentials to study  
454 cognition: recording standards and publication criteria. *Psychophysiology* **37**, 127–  
455 152 (2000).
- 456